J Solid State Electrochem (2016) 20:2461–2470
DOI 10.1007/s10008-016-3144-4

ORIGINAL PAPER

Solvent effects on the photoelectrochemical properties of WO_3 and its application as dopamine sensor

S. A. Alves[1] · L. L. Soares[1] · L. A. Goulart[1] · L. H. Mascaro[1]

Received: 23 October 2015 / Revised: 23 January 2016 / Accepted: 27 January 2016 / Published online: 5 February 2016

Abstract Nanostructured WO_3 films were produced by a simple method using ammonium tungstate dissolved in different solvents: ethanol, PEG 300, and a mixture of ethylene glycol with PEG 300. The suspensions were deposited on an FTO substrate by drop casting method and calcined at 500 °C in air atmosphere. The films were characterized by scanning electron microscopy (SEM), energy-dispersive X-ray spectroscopy (EDS), X-ray diffraction (XRD), UV–Vis diffuse reflectance spectroscopy, and photoelectrochemistry measurements. FTO substrates were fully covered by a thin and adherent WO_3 film, which presented a nanostructure with particle diameter of 30–80 nm. XRD confirms the monoclinic structure of WO_3. Ethanol samples presented higher photocurrent for water oxidation, compared to other solvents. However, these electrodes showed high fragility and the response did not present repeatability. High adhesion was obtained with PEG as solvent (by itself or mixed with ethylene glycol). In addition, WO_3 was applied as a photoelectrochemical sensor to detect dopamine under visible light irradiation. The developed sensor showed photosensitivity to dopamine with reproducibility, stability, wide linear range, and low detection limit (0.30 μM).

Keywords Tungsten oxide · Synthesis · Water splitting · Dopamine photoelectrochemical sensor

✉ L. H. Mascaro
lmascaro@ufscar.br

[1] Universidade Federal de São Carlos, Rodovia Washington Luiz, km 235, São Carlos, SP, Brazil

Introduction

Hydrogen has been considered outstanding as a clean energy carrier, and it can be used in different types of industries as well as in fuel cells. It can be produced by various methods, such as steam reforming. However, this method produces hydrogen with carbon emission which can cause environmental damage and fuel cell poisoning [1]. Hydrogen can be produced alternatively from photo(electro)chemistry systems using water. This process can produce hydrogen without presenting the challenge of unwanted emissions at the point of conversion, and the required energy can be acquired from sunshine. Thus, hydrogen can be obtained from a renewable energy source such as solar energy [2, 3].

Photoelectrochemical (PEC) solar cell is a device capable of splitting water into hydrogen and oxygen using a source of electrons. A major challenge for applying this kind of cell is the development of photoelectrodes that should present several properties, for example absorption of the solar radiation (especially visible radiation), photocorrosion stability, good efficiency, and cost-effectiveness [4–6].

Several materials have been studied for water splitting application. Between them, photocatalytic nanostructures are promising due to the small size, low recombination rates, and high crystallinity. Because of these factors, they present high efficiency [7–10]. Among semiconductor materials, tungsten oxide (WO_3) exhibits excellent performance in photoelectrochemical applications. It is an n-type semiconductor and presents favorable physical and chemical properties, such as small band gap (2.6–3.0 eV), chemical stability in acidic solutions, and resistance to photocorrosion. Thereby, WO_3 has been applied in gas sensors, catalysis, electrochromic devices, and photoelectrochemical cells [11, 12]. This material presents low cost as a benefit, when compared to noble materials. Another interesting property of WO_3

is polymorphism, (triclinic, monoclinic, orthorhombic, tetragonal, hexagonal, cubic phases) [13].

The main applied phases are hexagonal and monoclinic (h-WO_3 and m-WO_3, respectively). The hexagonal phase has been widely used in gas sensors due to its open-tunnel structure and rich intercalation with specific cations (Li^+, for example). m-WO_3 has been applied in photocatalytic processes using solar irradiation because this phase presents suitable band gap energy for the absorption of visible light [14].

In this sense, the synthesis method for m-WO_3 is very important, especially regarding the control of nanostructures size. The photocatalytic activity of WO_3 in water splitting application is directly related to the nanostructure and morphology of the prepared samples [14]. This phase is thermodynamically stable at room temperature, and so, it has been obtained by several methods, for example acid precipitation [15], sol–gel [16], electrodeposition [17], hydrothermal [18], hot-wire chemical vapor deposition [19], and electrospinning [20]. These methods have provided WO_3 nanoparticles with high photocatalytic efficiency; however, the syntheses have long time lengths or use aggressive chemical reagents. Santato et al. proposed a synthesis of WO_3 from Na_2WO_4. The Na_2WO_4 aqueous solution was passed through a proton exchange resin. Thus, tungstic acid was obtained, which was collected in ethanol. The solution was partially evaporated, and an organic stabilizer was added to solution. Among the main organic stabilizers tested, polyethylene glycol (PEG 300) was the most effective when compared to mannitol, ethylene glycol, and glycerol [21].

PEG has been used in different syntheses, in particular for WO_3 films. This organic reagent is known for increasing the inner surface area and developing morphology. Moreover, PEG can provide films with high porosity [22]. Ham D.J. et al. carried out WO_3 nanorods synthesis using PEG and the hydrothermal method [23]. Nanostructured WO_3 platelets were produced by Yagi M. et al. using ammonium tungstate, ethanol, and PEG to obtain a precursor paste. This paste was placed on ITO substrate using the doctor blade technique [24]. Yang H. et al. studied electrochromic and optical properties of WO_3 films produced by dip-coating pyrolysis. The precursor solution was a mixture of PEG, ammonium metatungstate, and water, which was aged at 40 °C for 12 h. The films were produced by the dip coating method and underwent pyrolysis at a furnace in air atmosphere [25].

A simple method based in a one-step preparation of a photoelectrode was proposed by Mascaro et al. [26]. $BiVO_4$ films were obtained by combination of $Bi(NO_3)_3$ and NH_4VO_3 directly in polyethylene glycol (PEG 300). This suspension was dropped in ITO-coated glass and calcined in air atmosphere. This method is simple and easy to employ because the suspension precursor is obtained by dissolving the salts in an organic stabilizer and the films are manufactured without requiring any instrumental apparatus (as in spin coating, dip coating, doctor blade, for example).

WO_3 is considered a versatile material due to its application in different areas. Among many applications, WO_3 is used as an electrochemical sensor. Multiwalled carbon nanotubes (MWCNTs) were used by Tsierkezos et al. to fabricate electrodes using the chemical vapor deposition technique with decomposition of either acetonitrile (ACN) or benzene (BZ) in the presence of ferrocene ($FeCp_2$) for DA detection. The detection limit obtained for the MWCNT-BZ electrode was 0.30 and 0.03 μM for the MWCNT-ACN electrode [27]. The same authors developed a sensor with phosphorus-doped multiwalled carbon nanotubes (P-MWCNTs). This film was grown on to oxidized silicon substrate in the presence of ferrocene using the chemical vapor deposition technique. The electrodes were successfully applied for the electrochemical detection of ascorbic acid (AA), dopamine (DA), and uric acid (UA). The limits of detection obtained were 1.12, 0.19, and 0.80 μM, respectively [28]. Yang et al. fabricated a functional nanocomposite of methylene blue on to the multiwalled nanotubes (MB-MWNTs). This modified electrode showed great electrocatalytic activity toward DA and UA. Peak separation between AA and DA was possible. The anodic peak current was linear to the concentration of DA in the range of 0.4–10.0 μM with a detection limit of 0.2 μM [29].

However, its application as photosensor is still in development, particularly in the determination of organic compounds. A sensor for dopamine was developed by Anithaa et al. using WO_3 nanoparticles with monoclinic (γ) and orthorhombic (β) structures. Glassy carbon electrode (GCE) was modified with WO_3 nanoparticles, and it was observed that γ-WO_3 nanoparticles showed an excellent electrocatalytic activity to dopamine (DA) oxidation in the presence of ascorbic acid (AA) at pH 7.0 without the presence of light. Differential pulse voltammetry (DPV) analysis showed that the electrode exhibited a linear response over a wide concentration range (0.1–600 μmol L^{-1}) of DA with the lowest detection limit of 24 nmol L^{-1} [30].

Recently, our research group has published a study using $BiVO_4$ photoanode as a photoelectroanalytical sensor for nitrite. The proposed sensor showed a wide range of detection (2.5–100.0 μmol L^{-1}), with a limit of detection of 1.5 μmol L^{-1} and reproducibility of 4.1 %. This new application for $BiVO_4$ is promising for the detection of inorganic species [31]. However, there are no studies reporting about this kind of photoelectrochemical sensor for organic compounds.

The aim of this study is to produce WO_3 films on FTO substrate using a simple synthesis method based in a modified sol-gel method. For this purpose, different solvents were evaluated: PEG 300, ethanol, and a mixture of ethylene glycol and PEG 300. The films were characterized by morphologic and structural techniques, and photocatalytic activity under visible

light was investigated. Furthermore, the application of WO_3 films as photoelectrochemical sensor for dopamine was evaluated.

Experimental

WO_3 film preparation

WO_3 films were produced by a modified sol-gel method using ammonium tungstate as precursor $[(NH_4)_{10}H_2(W_2O_7)_6]$ which was dissolved in different solvents: ethanol, polyethylene glycol (PEG 300), and a mixture of ethylene glycol + PEG 300 (1:4 *v*/*v*). All suspensions were sonicated for 30 min. Different concentration values were evaluated for the precursor: 0.01 and 0.03 M according to Table 1. The suspensions were deposited on the FTO substrate by drop casting method (5 μL cm^{-2}, total area of 1.0 cm^2) for the formation of one layer. Films were made with up to four layers, and after each deposition, the films were dried at 170 °C and the calcination was carried out at 500 °C for 5 h in air atmosphere. The substrates were fully covered with an adhesive yellow film after the preparation process.

Characterization

The morphologies and sizes of the WO_3 particles obtained were observed with a field emission scanning electron microscope (ESEM-FEG, FEI Inspect F 50). The crystalline structures of the samples were measured by X-ray diffraction (XRD) patterns obtained with a XRD 6000 Shimadzu diffractometer with Cu Kα radiation over the range of $10° \leq 2\theta \leq 70°$. The W/O ratio was determined by energy-dispersive X-ray spectroscopy (EDX) using an energy-dispersive X-ray spectrometer (EDAX, EDX-GENESIS). The band gap energy (E_g) was determined by means of UV–Vis diffuse reflectance absorption spectroscopy of the WO_3 samples using a Shimadzu UV spectrophotometer.

Table 1 Samples prepared from different solvents and precursor concentrations

Sample	Solvent	Precursor concentration
W_{ET-1}	Ethanol	0.01 M
W_{PEG-1}	PEG 300	0.01 M
$W_{EG/PEG-1}$	Ethylene glycol + PEG 300	0.01 M
W_{ET-3}	Ethanol	0.03 M
W_{PEG-3}	PEG 300	0.03 M
$W_{EG/PEG-3}$	Ethylene glycol + PEG 300	0.03 M

Photoelectrochemical assays

Photoelectrochemical measurements were carried out in a cell with three electrodes: a Pt auxiliary electrode, an Ag/AgCl/KCl saturated reference electrode and a working electrode. Na_2SO_4 (0.5 M) was used as the electrolyte. The photoelectrocatalytic activity of the electrodes was measured using solar simulator 500 W Xenon (Newport, 66902) calibrated to 100 mW cm^{-2}. Films were illuminated from the front and back side. Cyclic voltammetry was performed in the potential range from 0.0 to 1.5 V with a scan rate of 20 mV s^{-1}. Moreover, assays were carried out with 0.5 M Na_2SO_4 in the presence of Na_2SO_3 with the light on. The final concentrations of Na_2SO_3 were 1.0×10^{-4}, 1.0×10^{-3}, and 2.5×10^{-3} M.

Photoelectrochemical sensor for DA

The WO_3 electrode was applied for the oxidation of 1.0×10^{-4} M DA in phosphate buffer solution (PBS) 0.1 M, pH 7.0. The dopamine voltammetric behavior was evaluated without and with light using a solar simulator 500 W Xenon (Newport, 66902) calibrated to 100 mW cm^{-2}. The electrodes were illuminated from the back side. Photoelectrochemical determination of DA was carried out using cyclic voltammetry (CV), and the experiments were done using a scan rate of 50 mV s^{-1} in the potential range from −0.2 to +1.0 V vs. Ag/AgCl/KCl saturated. All cyclic voltammograms were performed under illumination. To obtain the calibration curves, aliquots of a standard solution of DA 1.0×10^{-3} M were added in 0.1 M PBS, pH 7.0. The detection limit (LOD) was calculated according to the IUPAC recommendation [32].

Results and discussion

Characterization of WO_3 films

WO_3 films were obtained using ammonium tungstate as precursor and different solvents (mixture of ethylene glycol + PEG 300, PEG 300, and ethanol). All films were calcined at 500 °C to obtain a crystalline material having photocatalytic properties and particle size in the nanometers scale. Ammonium tungstate can go through pyrolysis to form WO_3 as follows:

$$(NH_4)_{10}H_2(W_2O_7)_6 \rightarrow 12\ WO_3 + 10\ NH_3 + 12\ H_2O \quad (1)$$

The initial suspensions presented white color, and the films showed yellow color which is characteristic of the formation of WO_3. An interesting aspect in the preparation of suspensions is that when ethanol is used as solvent, the suspension is unstable and easily decants over time. Moreover, it is only possible to use this suspension on the same day of its

preparation. On the other hand, suspensions prepared with PEG 300 showed high stability and could be used in up to 7 days when kept in the refrigerator. Furthermore, suspensions put in the refrigerator are more easily manipulated since the viscosity decreases with PEG temperature. Thus, the manufacture of films by dripping the suspensions is improved. The use of precursor suspension with PEG instead of paste, for example, improves the reproducibility of the films produced.

WO_3 films produced from ammonium tungstate and ethylene glycol showed low adhesion with the substrate; these films easily leached in the solution. Despite the high solubility in this solvent, the fragility of the samples produced did not motivate the use of such suspension. Thus, assays were carried out with a mixture of ethylene glycol and PEG 300.

Morphologies of the WO_3 films were investigated by scanning electron microscopy (SEM). Figure 1a–c shows the top view images of W_{ET-3}, W_{PEG-3}, and $W_{EG/PEG-3}$ films, respectively. When ethanol was used as solvent (Fig. 1a), the film did not cover the entire surface of the substrate and it was possible to observe several cracks. Moreover, the surface morphology of this film showed agglomerated particles. Figure 1b shows an image of the film produced with PEG as solvent. This film had covered the FTO substrate but homogeneity was not observed. Spherical nanoparticles were predominant in this morphology and some large particles were observed as well. Finally, the film produced with a mixture of ethylene glycol and PEG 300 was homogeneous, consisting of uniform spherical nanoparticles with average particle diameter of 30 nm. Furthermore, the mixture solvent provided full coverage of the substrate.

The chemical composition of the films formed was confirmed by EDS analysis (Fig. 1d). From the spectra presented, strong W and O signals are observed for the sample using PEG 300 as solvent. The other samples showed similar composition, mainly containing W and O.

The formation of the WO_3 crystalline structure was verified by powder X-ray diffraction. Figure 2a shows the crystalline structure of the film calcined at 500 °C for 5 h for W_{PEG-1} sample. The majority of the diffraction peaks can be connected to WO_3 monoclinic phase, 23.07, 23.60, and 24.40 (PDF No. 43–1035). Besides, it is possible to observe other diffraction peaks which can be associated to the FTO substrate (SnO_2, PDF No. 88–287), these peaks are identified with a circle symbol. In

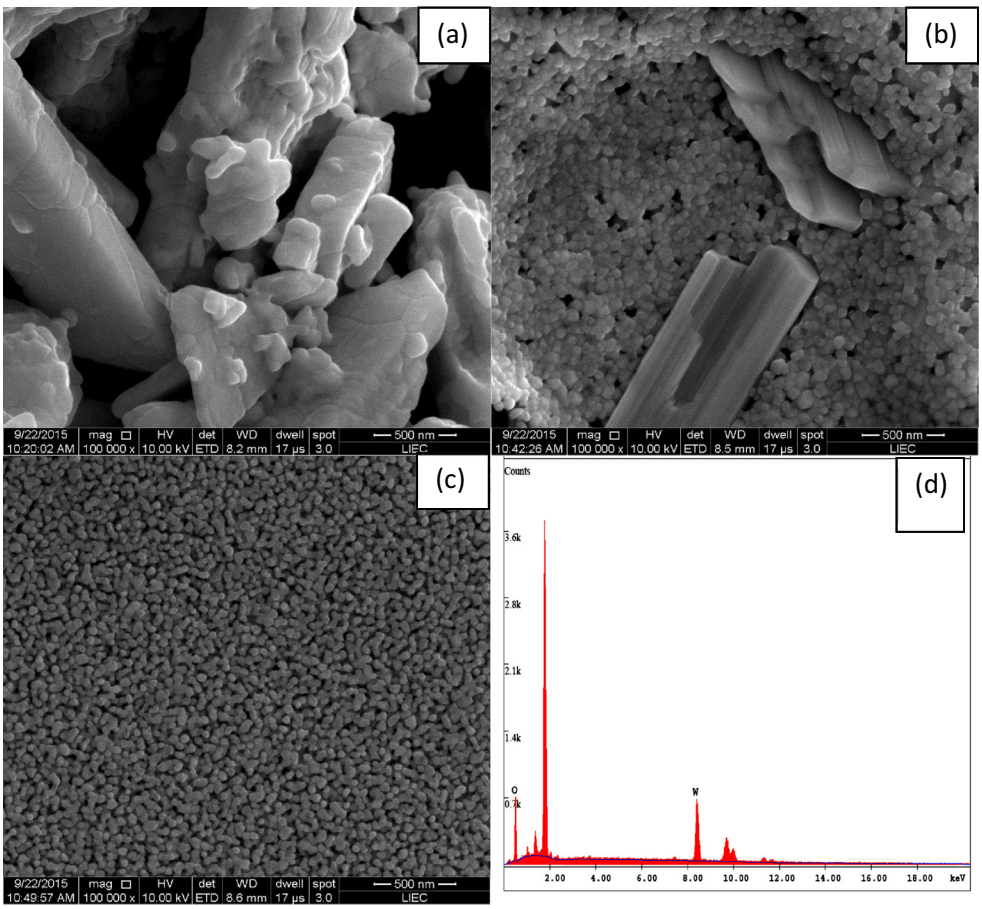

Fig. 1 FE-SEM images of the WO_3 films prepared from different solvents **a** W_{ET-3}, **b** W_{PEG-3}, **c** $W_{EG/PEG-3}$, and **d** EDS analysis

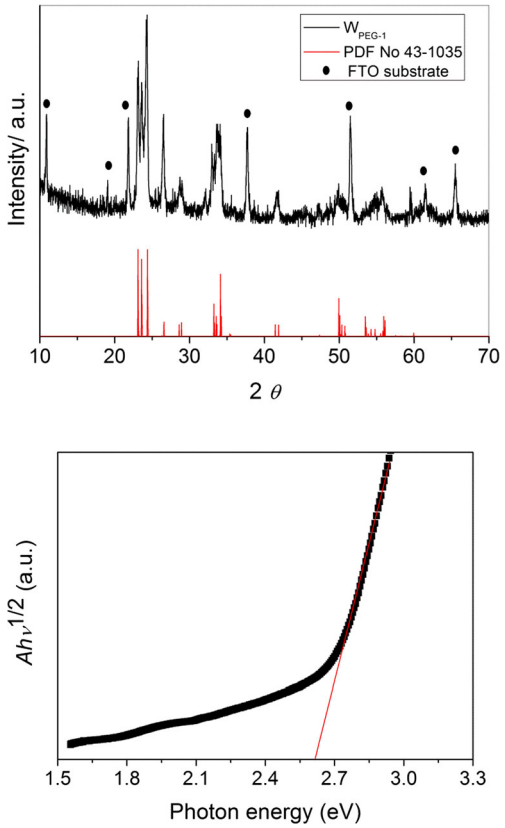

Fig. 2 **a** XRD patterns of the sample W_{PEG-1} on FTO substrate and **b** plot $\alpha h\nu^2$ vs. photon energy for a W_{PEG-1} sample from diffuse reflectance spectrum

every sample, the formation of the WO_3 crystalline structure was observed at 500 °C.

The WO_3 films optical properties were analyzed by diffuse reflectance spectroscopy. This measurement can be used to estimate the band gap energy (E_g) considering that WO_3 presents an indirect band gap according to Fig. 2b. The band gap energy was calculated from the equation for indirect allowed transitions:

$$\alpha h\nu^{1/2} = A(h\nu - Eg) \quad (2)$$

where α is the absorption coefficient at photon energy, $h\nu$, and A is a constant. The band gap can be estimated as 2.65, 2.60, and 2.60 eV for samples W_{ET-1}, W_{PEG-1}, and $W_{EG/PEG-1}$, respectively. These values are in agreement with the expected value for the band gap of the WO_3 monoclinic phase (2.6–2.90 eV).

Photocurrent measurements

The photocurrent of the WO_3 films can be an indicative of the photocatalytic activity in a photoelectrochemical cell. Figure 3 shows cyclic voltammograms for the $W_{EG/PEG-3}$ electrode on

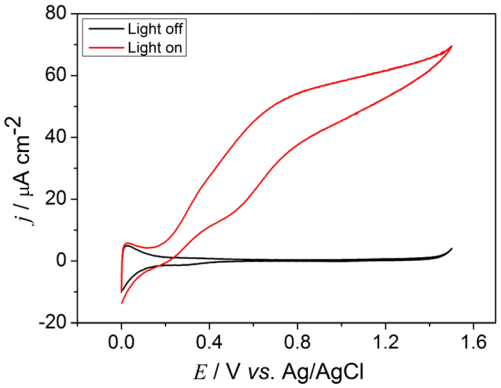

Fig. 3 Cyclic voltammogram for the $W_{EG/PEG-3}$ sample in 0.5 M Na_2SO_4 in the dark and light with scan rate of 20 mV s^{-1}

FTO in aqueous 0.5 M Na_2SO_4 solution in the dark and with frontal illumination (illumination of 100 mW cm^{-2}).

The redox system H_xWO_3/WO_3 was observed near 0.0 V. It is observed that anodic photocurrent increases from +0.16 V according to the potential application when under illumination. This is can be associated with the photooxidation of water, i.e., oxygen evolution. This result was expected since it is known that WO_3 is an n-type semiconductor, and it has been considered suitable for efficient photocatalytic oxidation. When the WO_3 film is illuminated, the electrons (e^-) from the valence band (E_v) are excited to the conduction band (E_c) leaving empty holes (h^+). The photoexcited electrons are taken to the auxiliary electrode (Pt), and they can be used to reduce H^+ to H_2. The holes can be used to promote water oxidation and produce O_2, according to equations:

$$WO_3 + h\nu \rightarrow WO_3(e^-_{CB}) + WO_3(h^+_{VB}) \quad (3)$$

$$4\ WO_3(h^+_{VB}) + 2H_2O \rightarrow O_2 + 4H^+ + 4\ WO_3 \quad (4)$$

The photocatalytic activity of the samples was evaluated considering the effect of the solvent and the concentration of the precursor salt, in accordance to photocurrent under solar simulator conditions (AM1.0), i.e., +0.71 V vs. Ag/AgCl at pH 5. Figure 4a, b shows photocurrent values for the precursor concentration of 0.01 M with front illumination and back illumination, respectively.

In general, it is noted that the photocurrent increases according to the solvent: ethanol > PEG 300 > ethylene glycol + PEG 300. Figure 4a shows the effects of increasing the number of layers and the different solvents. Thus, when ethanol is used, the photocurrent is higher compared to PEG 300 and ethylene glycol + PEG 300 for any number of layers studied (one to four layers). This behavior can be explained when FE-SEM images are observed. Because of the cracks in the film using ethanol as solvent, a higher surface area is expected and, consequently, greater photoelectrochemical response is expected. With electrodes of one, three, and four layers, the second best solvent is PEG 300. However, the electrode with

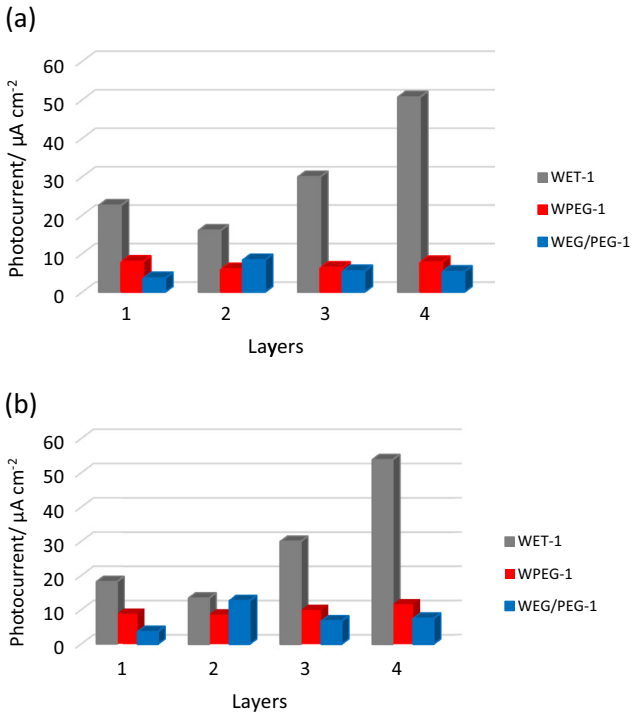

Fig. 4 Photocatalytic activity of the WO_3 samples for water splitting to form oxygen under UV–Vis irradiation with precursor concentration of 0.01 M: **a** front illumination and **b** back illumination

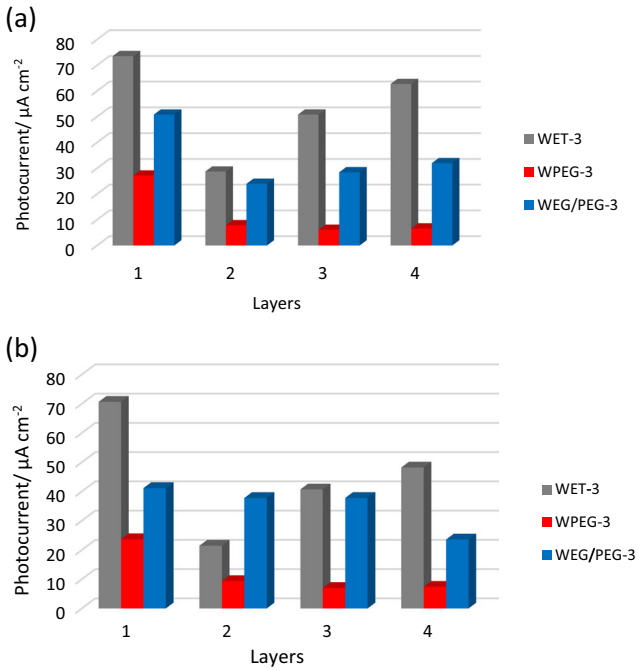

Fig. 5 Photocatalytic activity of WO_3 samples for water splitting to form oxygen under UV–Vis irradiation with precursor concentration of 0.03 M: **a** front illumination and **b** back illumination

two layers deposited and obtained with the ethylene glycol and PEG 300 mixture as solvent presented photocurrent greater than the electrode in which only PEG was used. Then, the films were illuminated from the back side, i.e., FTO substrate. Again, it is possible to observe that films produced with ethanol have greater photocurrent when compared to other solvents. The behavior of two layers was similar to the front illumination behavior. The photocurrent of the film obtained from mixed ethylene glycol + PEG 300 was close to response of the film obtained from ethanol. In addition, it is noticed that illumination from the front or back side has little effect on the photocurrent response for a precursor concentration of 0.01 M.

When the precursor concentration was 0.03 M (Fig. 5a, b), the same tendency is observed: the photocurrent is higher with ethanol as solvent. However, the second best solvent was the mixture of ethylene glycol + PEG 300, followed by PEG 300. The electrode with two layers of precursor and using the mixture of ethylene glycol + PEG 300 presented higher photocurrent than the ethanol and PEG 300 case. The effect of front and back illumination is more pronounced at 0.03 M precursor concentration, in this case back side presented higher photocurrent than front side illumination.

Although the ethanol samples presented higher photocurrent for water oxidation, these electrodes showed high fragility. WO_3 did not adhere to the substrate and was leached into the solution (solution presented yellow color). In addition, the response did not present repeatability, i.e., when several cyclic voltammetries were carried out with the same electrode, the photocurrent decreased. High adhesion is obtained with PEG as solvent, and the films obtained with PEG have repeatability and reproducibility. The use of ethylene glycol and PEG provided the best solubility for ammonium tungstate (promoting greater photocurrent at the highest concentration) and allowed the synthesis of a film with transparent and homogenous appearance. When only PEG is used as solvent, the film is opaque and the dissolution ammonium tungstate is lower and the preparation of the suspension is harder. The films with 0.03 M precursor concentration are more homogenous than the ones with 0.01 M, and they cover the substrate more easily.

The recombination processes of the WO_3 electrode were investigated using sulfite ions (Na_2SO_3). Figure 6 shows cyclic voltammograms of the $W_{EG/PEG-3}$ electrode in 0.5 M Na_2SO_4 with the light off and on and in sulfite presence (concentrations of 1.0×10^{-4} and 1.0×10^{-3} M).

Some species are able to react with holes from the photoexcited electrode to give SO_4^{2-} and, then, recombination processes in solution can be suppressed. Sulfite can be employed to act as a hole scavenger. Here, this effect can be observed due to the photocurrent increase according to the increase of the sulfite concentration (1.0×10^{-4} and 1.0×10^{-3} M). Moreover, a decrease in the onset potential (potential close to 0.0 V vs. Ag/AgCl) is noted. This behavior is a characteristic of the presence of a hole scavenger. Thereby, sulfite ions

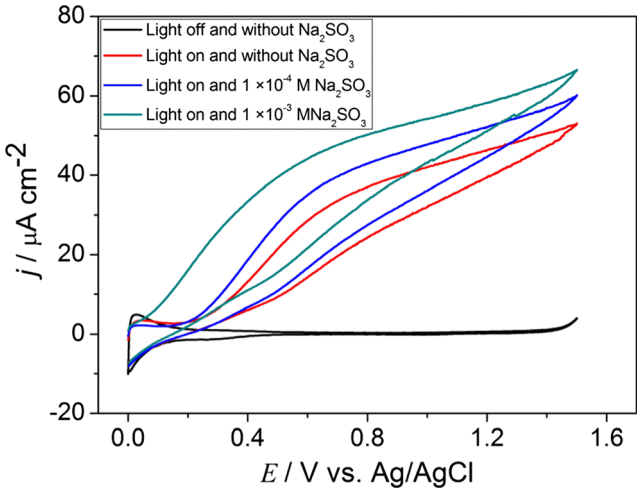

Fig. 6 Cyclic voltammetry of $W_{EG/PEG-3}$ film electrode in 0.5 M Na_2SO_4 without light, light on and the absence of Na_2SO_3 and in the presence of Na_2SO_3 (concentrations of 1.0×10^{-4} and 1.0×10^{-3} M)

have the function of hole scavengers, minimizing the recombination effect on the semiconductor surface leading to the rise of the photocurrent.

Application of WO_3 film as photoelectrochemical sensor for DA

The photosensor activity of the $W_{EG/PEG-3}$ electrode was demonstrated by comparison of cyclic voltammograms obtained, under light and at dark, of the 1.0×10^{-4} M DA solution in PBS 0.1 M, pH 7.0, Fig. 7a.

In the dark and with addition of DA, there is a current associated with the oxidation of dopamine but with very small value (4 μA cm^{-2}). When the $W_{EG/PEG-3}$ electrode is illuminated and in the presence of DA, the current density increases to 25.0 μA cm^{-2}, which is almost six times higher than the current observed in the dark. This result shows that the sensitivity of the sensor increases with the incidence of light (Fig 7b). Therefore, the use of WO_3 as photosensor would be more appropriate than its use only as sensor, as reported in the literature. Another important result is that the DA oxidation process starts in more negative potential when WO_3 is lit, showing the photoeletrocatalytic property of this material for this reaction. Under dark condition, the current associated to DA oxidation is lower because the kinetics of charge transfer at the WO_3 interface, the faradic process, is slower. However, under illumination, the DA oxidation process occurs due to the faradaic process and the presence of electron-hole pairs; in this way, the kinetics of charge transfer is faster increasing the photocurrent. Thus, the WO_3 electrode was used for the determination of dopamine by photocurrent measurement using cyclic voltammetry. Figure 8 presents the

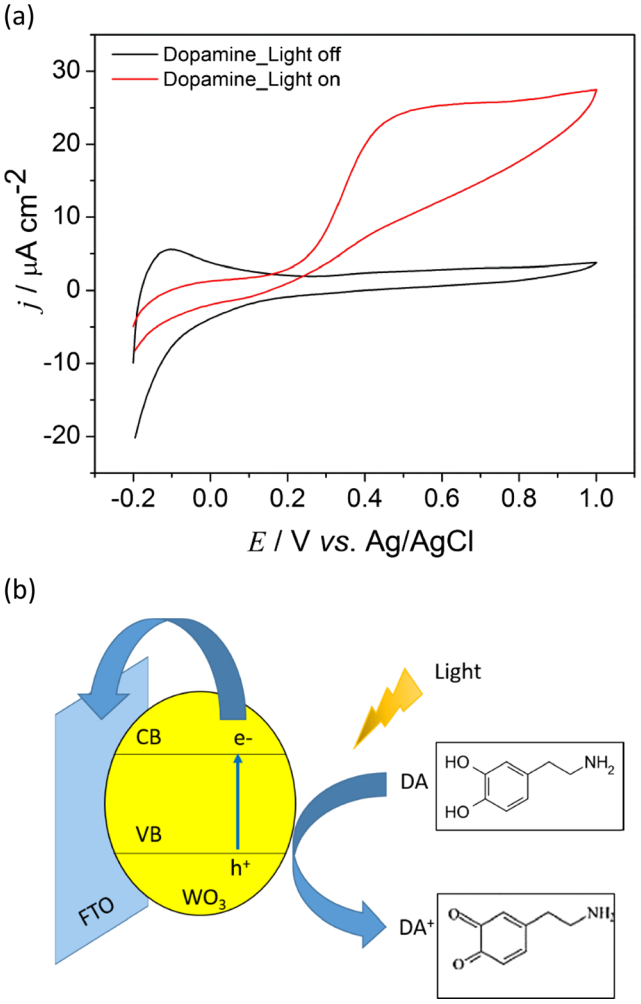

Fig. 7 **a** Cyclic voltammograms obtained at the $W_{EG/PEG-3}$ electrode in 0.1 M PBS pH 7.0 solution at a scan rate of 20 mV s^{-1} under light and dark conditions in the presence of 1.0×10^{-4} M DA and **b** schematic representation of DA oxidation in the FTO/WO_3 electrode

effect of different concentrations of DA on the photocurrent response of WO_3.

It can be observed that the photocurrent increased with the increasing of DA concentration (inset Fig. 8) and that there are two linear ranges, the first is a narrow linear range from 53 to 80 μM, the second linear range is from 85 to 155 μM. The correlation coefficients were 0.995 and 0.998, respectively. Thus, the present electrode shows a good linear response for the photoelectrochemical detection of DA in the range of 53–155 μM. The detection limit of the WO_3 sensor was determined to be 0.30 μM ($S/N = 3$). Compared with some previous reports for photosensors using chronoamperometry for DA determination, this work shows lower detection limit (Table 2). The effect of light on the electrochemical response for the detection of dopamine is evident because there is an increase in the electrode sensitivity and better resolution of the oxidation peak. Moreover, in the absence of light, the linear increase of current according to

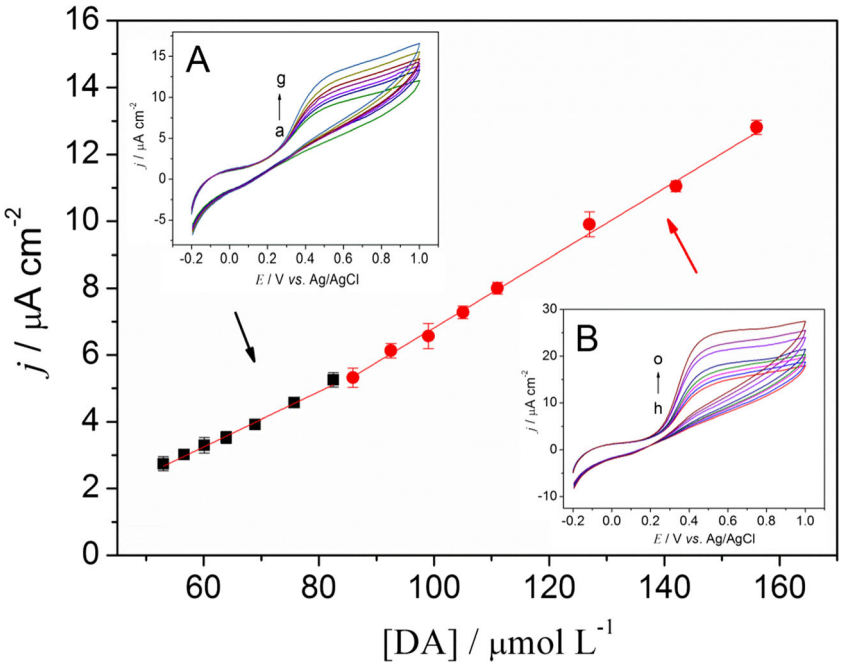

Fig. 8 Calibration plot of the current vs. concentration of DA (53.0 to 155 μM). *Insets* are cyclic voltammograms of DA with increasing concentration (*inset A* from *a* to *g*: 53.0, 56.6, 60.1, 63.9, 68.9, 80.0 μM; *inset B* from *h* to *o*: 85.0, 92.5, 99.0, 105.0, 111.0, 127.0, 142.0, 155.0 μM)

increased concentration was not observed. It is important to note that in the literature, there are quite sensitive sensors for dopamine; however, there are few studies that use photosensors to detect it due to this area being relatively new and unexplored. Thus, our results are very promising and may contribute to the development of this area.

Conclusions

In this study, a simple method for producing WO_3 films was demonstrated. The films were produced on FTO substrate using a one-step process based on the formation of an ammonium tungstate suspension in different solvents (ethanol, PEG 300, and a mixture of ethylene glycol + PEG 300) with calcination in air atmosphere. FTO substrate was fully covered by a thin and adherent WO_3 film. Moreover, WO_3 presented monoclinic structure. In general, it is noticed that photocurrent increases according to the solvent: ethanol > PEG 300 > ethylene glycol + PEG 300 to both precursor concentrations that were tested. However, electrodes produced with ethanol as solvent showed high fragility with WO_3 leaching into the solution. The film adhesion is obtained using PEG as solvent (alone or mixed with ethylene glycol), and the films obtained using such solvent have repeatability and reproducibility. The solubility of ammonium tungstate is higher in the presence of ethylene glycol. From this study, it was concluded that WO_3 synthesis on FTO substrate is promising for photoelectrochemical applications, such as water splitting. In addition, the WO_3 electrodes were highly photosensitive to dopamine, with

Table 2 Performance comparison of WO_3 photosensor for DA detection with other sensors

	Electrode	Linear range (μM)	Detection limit (μM)	Ref
Sensor	RuOx–Nf–GC	50 to 1100	5.0	[33]
	Poly(caffeic acid)-GC	1.0 to 40	0.40	[34]
	(MCPE)-Carbon Paste Electrode	8.0 to1400	0.84	[35]
	(Si/Db/CuTsPc)-carbon paste electrode	1.0 to 107	0.42	[36]
Photosensor	CdS QDs/ITO	0.02 to 50, 0.002 to 10	0.008	[37]
	TiO_2NPs/ITO	5.0 to 200, 200 to 5000	2.0	[38]
	WS_2/TiO_2/ITO	0.9 to 48.7, 72.2 to 333.3	0.32	[39]
	QDs/ITO	0.4 to 1000	0.17	[40]
	GQDs–TiO_2/GCE	0.02 to 105	0.006	[41]
	$W_{EG/PEG-3}$	53 to 80, 85 to 155	0.30	This work

a detection limit of 0.30 μM. Also, the electrode was verified as a promising photoelectrochemical sensor with stability, reproducibility, and a wide linear range of concentrations.

Acknowledgments The authors would like to thank FAPESP (Process 2014/10757-4 and 2015/ 00231-8), CEPID/FAPESP (Process No. 2013/07296-2), CNPq and CAPES for the financial support.

References

1. Maeda K, Domen K (2010) Photocatalytic water splitting: recent progress and future challenges. J Phys Chem Lett 1:2655–2661
2. Chen X, Shen S, Guo L, Mao SS (2010) Semiconductor-based photocatalytic hydrogen generation. Chem Rev 110: 6503–6570
3. A a I, DW B (2014) Photochemical splitting of water for hydrogen production by photocatalysis: a review. Sol Energy Mater Sol Cells 128:85–101
4. Yang J, Wang D, Han H, Li C (2013) Roles of cocatalysts in photocatalysis and photoelectrocatalysis. Acc Chem Res 46: 1900–1909
5. Paracchino A, Laporte V, Sivula K, Grätzel M, Thimsen E (2011) Highly active oxide photocathode for photoelectrochemical water reduction. Nat Mater 10:456–461
6. Osterloh FE (2013) Inorganic nanostructures for photoelectrochemical and photocatalytic water splitting. Chem Soc Rev 42:2294–2320
7. Chen HM, Chen CK, Liu R-S, Zhang L, Zhang J, Wilkinson DP (2012) Nano-architecture and material designs for water splitting photoelectrodes. Chem Soc Rev 41:5654–5671
8. Asai R, Nemoto H, Jia Q, Saito K, Iwase A, Kudo A (2014) A visible light responsive rhodium and antimony-codoped SrTiO3 powdered photocatalyst loaded with an IrO2 cocatalyst for solar water splitting. Chem Commun (Camb) 50:2543–2546
9. Chen Z, Cummins D, Reinecke BN, Clark E, Sunkara MK, Jaramillo TF (2011) Core-shell MoO 3-MoS 2 nanowires for hydrogen evolution. Nano Lett 11:4168–4175
10. Chou J-C, Yang M-H, Liao J-W, Lee C-Y, Gan J-Y (2014) Photoexcitation of TiO2 photoanode in water splitting. Mater Chem Phys 143:1417–1422
11. Nandiyanto ABD, Arutanti O, Ogi T, Iskandar F, Kim TO, Okuyama K (2013) Synthesis of spherical macroporous WO3 particles and their high photocatalytic performance. Chem Eng Sci 101:523–532
12. Zhao Y, Wei X, Wang Y, Luo F (2014) One-pot twelve tungsten phosphate acid assisted electrochemical synthesis of WO3-decorated graphene sheets for high-efficiency UV-light-driven photocatalysis. Chem Phys Lett 607:34–38
13. Szilágyi IM, Fórizs B, Rosseler O, et al. (2012) WO3 photocatalysts: influence of structure and composition. J Catal 294:119–127
14. Hernandez-Uresti DB, Sánchez-Martínez D, Martinez-de la cruz A, Sepúlveda-Guzmán S, Torres-Martínez LM (2014) Characterization and photocatalytic properties of hexagonal and monoclinic WO3 prepared via microwave-assisted hydrothermal synthesis. Ceram Int 40: 4767–4775
15. Luévano-Hipólito E, Martínez-de la Cruz A, Yu QL, Brouwers HJH (2014) Precipitation synthesis of WO3 for NOx removal using PEG as template. Ceram Int 40:12123–12128
16. Caruso T, Castriota M, Policicchio A, et al. (2014) Thermally induced evolution of sol–gel grown WO3 films on ITO/glass substrates. Appl Surf Sci 297:195–204
17. Qi C-X, Tan Z, Feng Z-H, Yu L-P (2014) Fabrication of bowl-like porous WO3 film by colloidal crystal template-assisted electrodeposition method. J Mater Sci Mater Electron 25:1553–1558
18. Shen Y, Yan P, Yang Y, Hu F, Xiao Y, Pan L, Li Z (2015) Hydrothermal synthesis and studies on photochromic properties of Al doped WO3 powder. J Alloys Compd 629:27–31
19. Houweling ZS, Harks P-PRML, Kuang Y, van der Werf CHM, Geus JW, Schropp REI (2015) Hetero- and homogeneous three-dimensional hierarchical tungsten oxide nanostructures by hot-wire chemical vapor deposition. Thin Solid Films 575:76–83
20. He Z, Liu Q, Hou H, Gao F, Tang B, Yang W (2015) Tailored electrospinning of WO_3 nanobelts as efficient ultraviolet photodetectors with photo-dark current ratios up to 1000. ACS Appl Mater Interfaces 150515092335006 7(20):10878–10885
21. Santato C, Odziemkowski M, Ulmann M, Augustynski J (2001) Crystallographically oriented mesoporous WO3 films: synthesis, characterization, and applications. J Am Chem Soc 123:10639–10649
22. Li YJ, Liu ZF, Liang XP, Ya J, Cui T, Liu ZC (2014) Synthesis and electrochromic properties of PEG doped WO 3 film. Mater Technol 29:341–349
23. Ham DJ, Phuruangrat A, Thongtem S, Lee JS (2010) Hydrothermal synthesis of monoclinic WO3 nanoplates and nanorods used as an electrocatalyst for hydrogen evolution reactions from water. Chem Eng J 165:365–369
24. Yagi M, Maruyama S, Sone K, Nagai K, Norimatsu T (2008) Preparation and photoelectrocatalytic activity of a nano-structured WO3 platelet film. J Solid State Chem 181:175–182
25. Yang H, Shang F, Gao L, Han H (2007) Structure, electrochromic and optical properties of WO3 film prepared by dip coating-pyrolysis. Appl Surf Sci 253:5553–5557
26. Mascaro LH, Pockett A, Mitchels JM, et al. (2014) One-step preparation of the BiVO4 film photoelectrode. J Solid State Electrochem 1–5 19(1):31–35
27. Tsierkezos NG, Ritter U (2012) Oxidation of dopamine on multi-walled carbon nanotubes. J Solid State Electrochem 16:2217–2226
28. Tsierkezos NG, Ritter U, Thaha YN, Downing C, Szroeder P (2015) Synthesis, characterization, and electrochemical application of phosphorus-doped multi-walled carbon nanotubes. J Solid State Electrochem 19:891–905
29. Yang SL, Li G, Yang R, Xia MM, Qu LB (2011) Simultaneous voltammetric detection of dopamine and uric acid in the presence of high concentration of ascorbic acid using multi-walled carbon nanotubes with methylene blue composite film-modified electrode. J Solid State Electrochem 15:1909–1918
30. Anithaa AC, Lavanya N, Asokan K, Sekar C (2015) WO3 nanoparticles based direct electrochemical dopamine sensor in the presence of ascorbic acid. Electrochim Acta 167:294–302
31. Ribeiro FWP, Moraes FC, Pereira EC, Marken F, Mascaro LH (2015) New application for the BiVO4 photoanode: a photoelectroanalytical sensor for nitrite. Electrochem Commun 61:1–4
32. Methods CA (1987) Recommendations for the definition, estimation and use of the detection limit. R Soc Chem 112:199–204
33. Ti CC, Kumar SA, Chen SM (2009) Electrochemical preparation, characterization, and electrocatalytic studies of Nafion-ruthenium oxide modified glassy carbon electrode. J Solid State Electrochem 13:397–406
34. Li NB, Ren W, Luo HQ (2008) Simultaneous voltammetric measurement of ascorbic acid and dopamine on poly(caffeic acid)-modified glassy carbon electrode. J Solid State Electrochem 12:693–699
35. Ardakani MM, Talebi A, Naeimi H, Barzoky MN, Taghavinia N (2009) Fabrication of modified TiO2 nanoparticle carbon paste electrode for simultaneous determination of dopamine, uric acid, and l-cysteine. J Solid State Electrochem 13:1433–1440

36. Deon M, Caldas EM, da Rosa DS, de Menezes EW, Dias SLP, Pereira MB, Costa TMH, Arenas LT, Benvenutti EV (2015) Mesoporous silica xerogel modified with bridged ionic silsesquioxane used to immobilize copper tetrasulfonated phthalocyanine applied to electrochemical determination of dopamine. J Solid State Electrochem 19(7):2095–2105
37. Wang G, Jiao H, Liu K, Wu X, Dong Y, Li Z, Zhang C (2014) Electrochemistry Communications Short communication A novel strategy for the construction of photoelectrochemical sensors based on quantum dots and electron acceptor : The case of dopamine detection. Electrochem Commun 41:47–50
38. Gao P, Ma H, Yang J, Wu D, Zhang Y, Du B, Fan D, Wei Q (2015) Anatase TiO_2 based photoelectrochemical sensor for the sensitive determination of dopamine under visible light irradiation. New J Chem 39:1483–1487
39. Ma W, Wang L, Zhang N, Han D, Dong X, Niu L (2015) Biomolecule-free, selective detection of o-diphenol and its derivatives with WS2/TiO2-based photoelectrochemical platform. Anal Chem 87:4844–4850
40. Hao Q, Wang P, Ma X, Su M, Lei J, Ju H (2012) Charge recombination suppression-based photoelectrochemical strategy for detection of dopamine. Electrochem Commun 21:39–41
41. Yan Y, Liu Q, Du X, Qian J, Mao H, Wang K (2015) Visible light photoelectrochemical sensor for ultrasensitive determination of dopamine based on synergistic effect of graphene quantum dots and TiO2 nanoparticles. Anal Chim Acta 853:258–264